Geochemical Journal, Vol. 44, pp. 379 to 386, 2010

Two types of adakites revealed by ^{238}U–^{230}Th disequilibrium from Daisen Volcano, southwestern Japan

SAIMI TOKUNAGA, SHUN'ICHI NAKAI* and YUJI ORIHASHI

Earthquake Research Institute, The University of Tokyo, 1-1-1 Yayoi, Bunkyo-ku, Tokyo 113-0032, Japan

(*Received September 19, 2009; Accepted March 4, 2010*)

Daisen volcano is located on the Quaternary volcanic front in southwestern Japan. The volcano is composed mainly of andesite and dacite, which chemically resemble adakites, with high Al_2O_3 and Sr/Y, steep REE patterns, and no negative Eu anomaly. ($^{238}U/^{230}Th$) disequilibrium (herein, a ratio in parentheses denotes the activity ratio) and trace element analyses of adakites from two volcanic domes, Karasugasen and Misen, indicate two adakite types. Adakite from Karasugasen is characterized by excess (^{230}Th) over (^{238}U), typical of most adakites, whereas adakite from Misen is characterized by excess (^{238}U) over (^{230}Th). The latter is consistent with enrichment in fluid-mobile elements relative to fluid immobile elements compared to rocks from Karasugasen. The values of ($^{230}Th/^{232}Th$) of adakites from Karasugasen and Misen are, respectively, around 0.75 and 0.81. These low ($^{230}Th/^{232}Th$) ratios result from the incorporation of subducted sedimentary material. The ratios, nevertheless, are higher than that for the estimate of lower crustal material suggesting significant incorporation of lower crust is unlikely. As adakites from Misen have (^{238}U) excess over (^{230}Th), adakite magma must have interacted with wedge mantle metasomatized by a slab-derived fluid, confirming the presence of a fluid-metasomatized mantle beneath Daisen volcano.

Keywords: adakite, U–Th radioactive disequilibrium, Daisen, slab melting, subduction

INTRODUCTION

Adakites typically have high Sr contents (>300 ppm, up to 2000 ppm), with strongly fractionated REE patterns, very low concentrations of Y and heavy rare earth elements (HREEs; Yb ≤ 1.8 ppm, Y ≤ 18 ppm), and lacking negative Eu-anomalies (Martin, 1999). Adakites result from the melting of a mafic source and are restricted to subduction zones (e.g., Martin, 1986; Defant *et al*., 1991; Defant and Drummond, 1990, 1993; Drummond and Defant, 1990). Therefore, adakite can be produced by melting of the subducting basaltic slab. Slab melting appears where a young, hot slab subducts and exceeds its solidus before it dehydrates. If adakitic magma forms in this way, there is a strong possibility that it will interact with the mantle wedge on its way to the surface. The influence of this interaction is reflected in MgO, Ni, and Cr enrichments (e.g., Martin, 1999). In contrast, Atherton and Petford (1993) argued that sodium-rich plutonic and vocanic rocks from the Cordillera Blanca complex in Peru, that have geochemical characteristics of adakite, formed by partial melting of newly underplated thick basaltic crust.

*Corresponding author (e-mail: snakai@eri.u-tokyo.ac.jp)

Volcanic rocks at Daisen volcano show typical features of adakite, such as high Sr contents, Sr/Y, and La/Yb ratios. Melting of the young Philippine Sea Plate (26–28 Ma), which extends beneath the volcano, is considered to account for the genesis of these adakitic rocks (Morris, 1995; Peacock and Wang, 1999). Peacock and Wang (1999) used thermal-petrologic models in a discussion of dehydration, magmatism and seismicity in northeastern and southwestern Japan, where cool and warm subduction take place, respectively. According to them, beneath southwestern Japan, most water in the subducting slab is dehydrated at shallow depths (<50 km) and is not available to trigger partial melting of the mantle wedge. An adakitic magma which ascends through wedge mantle can be used as a probe to investigate geochemical charagteristics of the wedge mantle. Interaction of an adakitic magma with the overlying mantle has been discussed where the mantle had suffered metasomatism by a slab-derived melt (Bourdon *et al*., 2002). The detection of hydrated wedge mantle at the point of generation of adakitic magma, however, would place some constraints on whether the mantle layer metasomatized by dehydration can be dragged into the volcanic front in southwestern Japan.

($^{238}U/^{230}Th$) disequilibrium studies can help understand recent magmatic process, such as the contribution of fluid to the generation of melt in subduction zones, because U and Th are both highly-incompatible elements and cannot be fractionated from each other during crystallization of common minerals during partial melting, although fractionation of U and Th can occur during dehydration, reflecting the different mobilities of the two elements in aqueous fluids (Turner *et al.*, 2003). Many basalts from oceanic island-arc environments, such as the Mariana and Izu arcs, show a distinct excess of (^{238}U) over (^{230}Th), indicating that magma genesis is triggered by dehydration of the subducting slab. In contrast, (^{238}U/^{230}Th) disequilibrium data for young adakites from the Andean Austral volcanic zone (Sigmarsson *et al.*, 1998), where the Chile ridge subducts beneath South America, show a uniform excess of (^{230}Th) over (^{238}U).

In this study, we examine the (^{238}U/^{230}Th) disequilibrium of adakites from the Karasugasen and Misen volcanic domes at Daisen volcano in order to investigate the nature of the sub-arc mantle where adakites form. Based on this knowledge, we then assess the geochemical character of the wedge mantle.

Geological Background and Samples

Daisen is a Quaternary arc volcano situated in southwest Japan, where it is associated with the subduction of the Philippine Sea Plate beneath the Eurasia Plate (Fig. 1). Daisen is a large composite volcano, more than 120 km^3 in volume, ranging in age from 0.017 to 1.2 Ma, and consisting of several clustered and overlapping lava domes (Kimura *et al.*, 2005; Tamura *et al.*, 2000, 2003; Tsukui, 1984, 1985; Tsukui *et al.*, 1985). Samples discussed here were collected from the Karasugasen and Misen lava domes. The Misen lava dome forms the summit of Daisen (1729 m), whereas the Karasugasen lava dome is located 3 km to the southwest. The first ash fall from the Karasugasen overlies the Aira–Tanzawa tephra, whose eruption age is about 26 ka (Tsukui, 1984). Misen eruption occurred at *ca*. 17 ka, which was the last eruption of Daisen (Tsukui, 1984).

Both lava domes are dacitic. Karasugasen consists of porphyritic dacite, with phenocrysts of plagioclase (15–20 vol.%), hornblende (5–10 vol.%), with or without minor quartz, biotite, or hypersthene. The Misen lava dome is less crystalline, with 5–10% plagioclase phenocrysts, and 1–3% phenocrysts of hornblende, biotite, hypersthene, and/or quartz. Kimura *et al*. (2005) and Tamura *et al*. (2000, 2003) reported geochemical data on the volcanic rocks from Daisen. ^{87}Sr/^{86}Sr and ^{143}Nd/^{144}Nd of Daisen dacites range between 0.7041 and 0.7052 and 0.51272 and 0.51278 (Tamura *et al*., 2000, 2003). The isotopic compositions are close to those of bulk earth (Zindler and Hart, 1986). Kimura *et al*. (2005) suggested that the Karasugasen dacite were derived from the slab sediment melting based on the isotopic data.

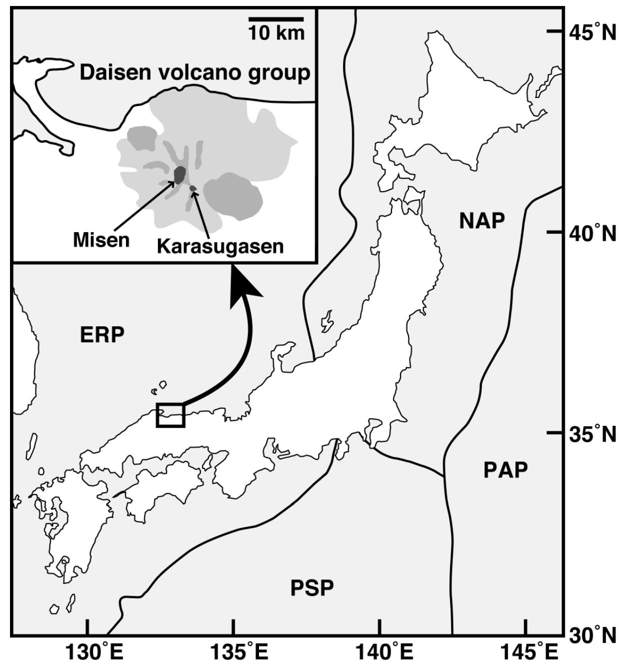

Fig. 1. Location map of Daisen volcano modified from Kimura et al. (2005). The inset figure shows an enlarged view of Daisen volcano. EPR, NAP, PAP, and PSP respectively stand for Eurasian Plate, North America Plate, Pacific Plate, and Philippine Sea Plate.

Analytical

Thirteen samples were crushed with an agate mortar, following washing in a Milli-Q water ultrasonic bath.

Major element data and trace element data except rare earth elements, U, Th were analyzed by X-ray fluorescence spectrometry (XRF) at ERI, the University of Tokyo, (PW2400; Philips Japan Ltd.) following the method described in Tani *et al*. (2002). The concentrations of the rare earth elements were determined using an ICP-MS fitted with a quadrupole mass analyzer at ERI (PQ3; Thermo Elemental, Winsford, U.K.). Accuracy and precision of the analyses are shown in Fukuda *et al*. (2008). RSD of most of the elements was better than 10%.

The analytical scheme for (^{238}U/^{230}Th) disequilibrium analysis has been described by Fukuda and Nakai (2002). U and Th were purified using anion exchange resin (AGX1-8; Bio-Rad Laboratories Inc.). Abundance measurements were carried out by isotope dilution analysis. A reagent of depleted U ($U(NO_3)_4$, 94270; Fluka Chemika GmbH) was used as a U spike. The ^{230}Th spike was prepared by separation of ^{230}Th from natural U. The abundance and isotope measurements were performed using a MC-ICPMS at ERI (IsoProbe; GV Instruments Ltd., Manchester, U.K.). An Aridus micro-concentric nebulizer (Cetac Technologies, Omaha, U.S.A.) was used to intro-

Table 1. *Geochemical chracteristics of adakite and the samples from Daisen volcano*

	Adakite*	Karasugasen	Misen
SiO_2 (wt%)	64.7 (3.2)	62.7–65.1	64.2–65.4
Al_2O_3 (wt%)	16.8 (1.0)	16.8–18.0	16.7–17.2
Y (ppm)	10 (4)	8–10	9–10
Yb (ppm)	0.93 (0.37)	0.55–0.69	0.59–0.68
Sr/Y	69	73–97	72–79
$(La/Yb)_N$**	14	11.3–22.6	12.8–19.5
Cr (ppm)	36 (34)	14–18	15–19
Ni (ppm)	24 (19)	9–18	8–16
Eu anomaly	positive	positive	positive

**Average chemical composition of adakites (n = 81) are from Martin (1999) with standard deviation in parenthesis.*
***Chondrite normalized ratio.*

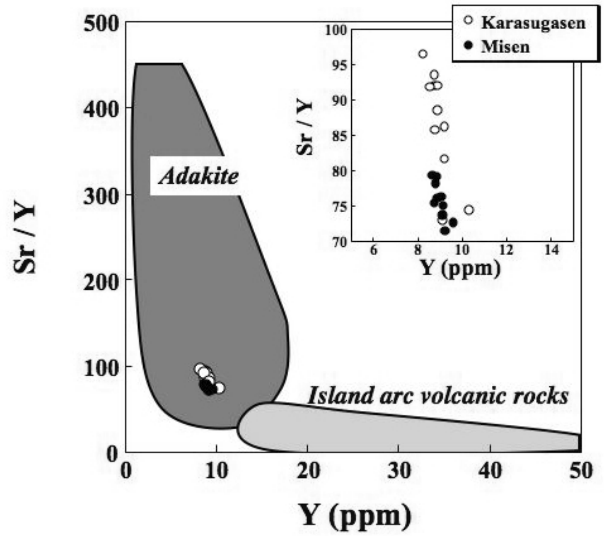

Fig. 2. Sr/Y vs. Y (ppm) for Daisen dacites. Fields for adakites and island arc volcanic rocks are from Drummond and Defant (1990). The inset figure shows an enlarged view for the samples from Daisen volcano.

duce the sample solutions. The errors for the ($^{230}Th/^{232}Th$) and ($^{238}U/^{232}Th$) ratio were estimated respectively as about 0.5% and 2% (Fukuda and Nakai, 2002). In this study we used the following decay constants for calculation of radioactivity ratios: ($\lambda^{238}{}_{U} = 1.551 \times 10^{-10}$ yr^{-1} (Jaffey *et al.*, 1971), $\lambda^{230}{}_{Th} = 9.158 \times 10^{-6}$ yr^{-1} (Cheng *et al.*, 2000), $\lambda^{232}{}_{Th} = 4.945 \times 10^{-11}$ yr^{-1} (Holden, 1990).

RESULTS AND DISCUSSION

Results of geochemical and U–Th radioactive analyses of Daisen adakites

Major element compositions (Table 1, Appendix 1) show that dacitic rocks from both lava domes are basically similar and overlap with compositions reported by Morris (1995). Trace element compositions of Karasugasen and Misen samples (Table 1, Appendix 1) are similar to other worldwide adakites (e.g., Martin, 1999), although adakaites from Karasugasen has higher Sr contents than those from Misen. They plot in the adakite field in terms of Sr/Y–Y (Fig. 2), and have steep REE patterns with positive Eu anomalies (Appendix 2, Fig. 3), which are typical of adakites. These results are consistent with previous reports for Daisen dacites (Morris, 1995; Kimura *et al.*, 2005). Cr and Ni abundances in the Dasisen adakites are lower compared with averages of adakites, which has been pointed out by Kimura *et al.* (2005).

The whole-rock ^{238}U–^{230}Th radioactive disequilibrium data of the Daisen samples are shown in Table 2 and an equiline diagram (Fig. 4). The ($^{230}Th/^{232}Th$) values for Karasugasen and Misen show a limited range from 0.71 to 0.79 and from 0.81 to 0.85, respectively. All values are quite lower than those for MORB and volcanic rocks typical of oceanic island-arcs, which have ratios grater than one. Lower ($^{230}Th/^{232}Th$) ratios result from the incorporation of surface crustal material introduced as subducting

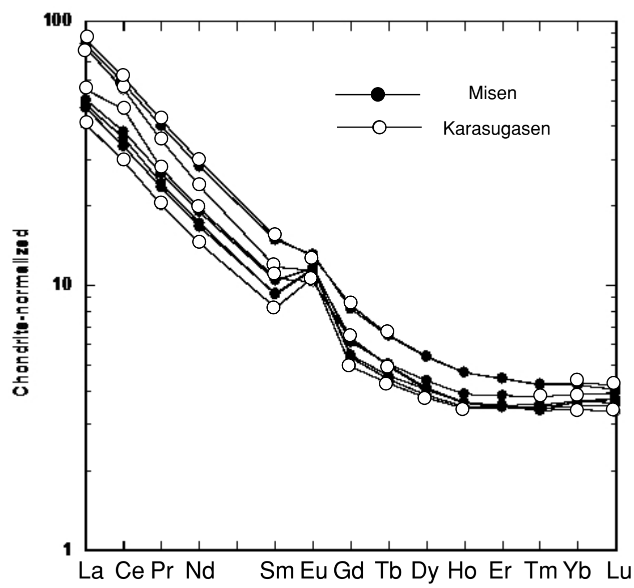

Fig. 3. Chondirite normalized REE patterns of Daisen adakites. CI abundances used for normalization are from McDonough and Sun (1995).

sediment. ($^{230}Th/^{232}Th$) of Karasugasen adakites in Fig. 4 are similar to that of global subducting sediments (GLOSS, Plank and Langmuir, 1998).

Most samples from Karasugasen show excess (^{230}Th) over (^{238}U), with ($^{230}Th/^{232}Th$) from 0.71 to 079. Sigmarsson *et al.* (1998) reported that young adakites

Table 2. U–Th radioactive disequilibria data of the samples from Daisen volcano

Dome	U (ppm)*	Th (ppm)*	Th/U	($^{238}U/^{232}Th$)	($^{230}Th/^{232}Th$)	($^{238}U/^{230}Th$)
Karasugasen						
K1	1.65	6.64	4.02	0.755	0.779	0.969
K2	1.63	6.63	4.07	0.746	0.748	0.997
K3	1.44	5.99	4.16	0.729	0.729	1.000
K4	1.20	7.18	5.98	0.508	0.704	0.722
K5	1.12	6.63	5.94	0.511	0.713	0.716
K7	1.33	6.52	4.89	0.620	0.746	0.832
K11	1.47	6.38	4.33	0.701	0.749	0.936
Misen						
M1	1.29	4.23	3.28	0.926	0.828	1.118
M2	1.15	4.34	3.77	0.804	0.815	0.986
M3	1.23	4.39	3.58	0.847	0.839	1.010
M6	1.07	3.87	3.61	0.840	0.803	1.045
M7	0.96	3.46	3.63	0.837	0.821	1.019
M10	1.27	4.51	3.55	0.855	0.806	1.060

Abundances were determined by isotope dilution method.

from the Andean Austral volcanic zone show a uniform excess of (^{230}Th) over (^{238}U), but variable Th isotope ratios for different volcanoes as shown in Fig. 4. Excess (^{230}Th) over (^{238}U) in an adakitic melt is generally explained by residual garnet in eclogite because $D_U > D_{Th}$ in garnet (Beattie, 1993; LaTourette *et al.*, 1993). Therefore, the excess of (^{230}Th) over (^{238}U) at Karasugasen is consistent with its origin from melting of eclogite leaving residual garnet. In contrast, the samples from Misen show an excess of (^{238}U) over (^{230}Th), which is typical of many arc systems such the Izu and Mariana arcs (Turner *et al.*, 2003), and the Southern Volcanic Zone in Chile (Fig. 4). The ($^{238}U/^{230}Th$) data imply that a fluid-related component derived from the subducting slab is involved in the genesis of the Misen magma.

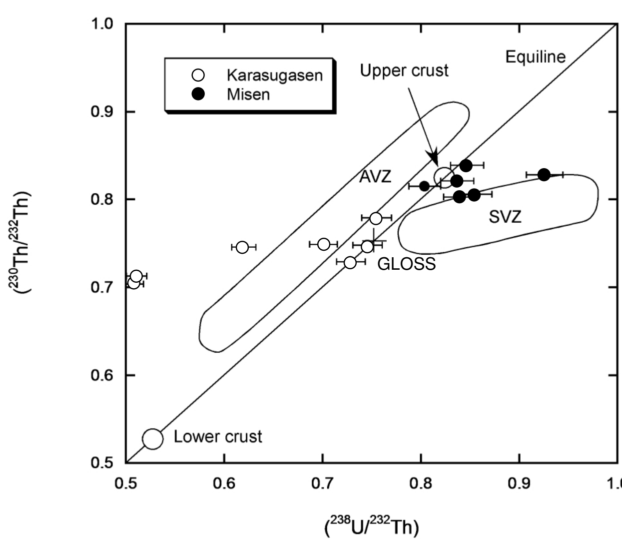

Fig. 4. ($^{230}Th/^{232}Th$)–($^{238}U/^{232}Th$) equiline diagram for Daisen adakites. No eruption time correction were made on ($^{230}Th/^{232}Th$). U–Th disequilibrium data for Austral Volcanic Zone and Southern Volcanic Zone of Andez are also shown (Sigmarsson et al., 1998). The estimate compositions of upper and lower crust (Rudnick and Gao, 2003) are shown with circles. Each value may contain uncertainty of 10–30%. U and Th composition of global subducting sediment (GLOSS) by Plank and Langmuir (1998) is shown as a cross.

U–Th constraints on the origin of Daisen adakites

Kimura *et al.* (2005) reported that the chemistry of the Karasugasen lava is similar to other Diasen–Hiruzen lavas that erupted over an interval of a million years. Because large amount of adakitic magma (>100 km^3) in the area requires a massive homogeneous source, they argued for slab melting as a plausible mechanism for the production of the Karasugasen adakites. Meanwhile, Iwamori (1991) suggested involvement of lower crust melting by mafic underplate. As far as we know, there exists no report on trace element and isotope data on lower crustal xenoliths in the Daisen area. The composition of average lower continental crust (Rudnick and Gao, 2003) was estimated to have Th/U ratio of 6.0. Melting of this material produces a magma with ($^{230}Th/^{232}Th$) of 0.52, if the material had attained radioactive equilibrium before melting. The ($^{230}Th/^{232}Th$) of the material, much lower than the observed values for the Daisen adakites, is not consistent with the lower crust origin of the adakites (Fig. 4). Shiomi *et al.* (2006) determined Moho depth at the coastline of the Sea of Japan as around 30 km based on receiver function inversion. Compared with the Cordillera Blanca complex in Peru where underplated thick basaltic crust was ascribed to genesis of adakite (Atherton and

Petford, 1993), the crustal thickness beneath Daisen is not enough for garnet of be stable. The crustal melting would not produce the Karasugasen adakites with the excess of (^{230}Th) over (^{238}U). Moreover, as Kimura *et al.* (2005) pointed out, REE patterns of Karasugasen adakites are not consistent with lower crustal melt origin. REE patterns of adakites from Misen (Fig. 3) are also similar to those reported by Kimura *et al.* (2005). We therefore argue for slab melting as more plausible mechanism.

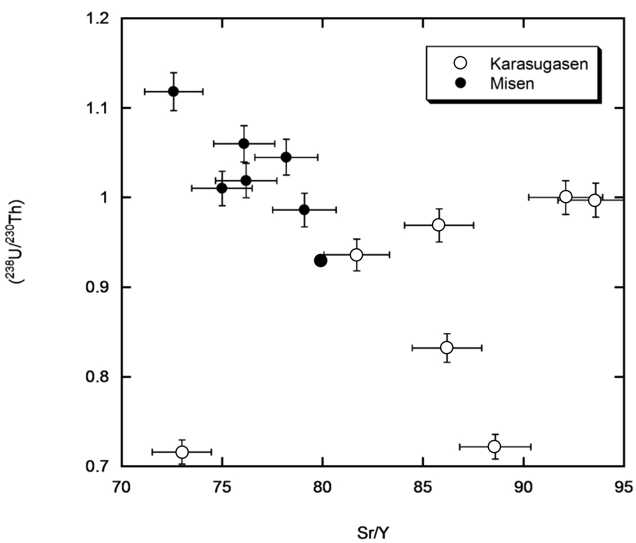

Fig. 5. Sr/Y–(^{238}U/^{230}Th) diagram of adakites from two edifices of Daisen volcano.

Origin of (^{238}U) excess over (^{230}Th) in Misen samples

Adakites from Misen have (^{238}U) excess over (^{230}Th) (Fig. 4). The (^{238}U/^{230}Th) ratios of samples from Misen are negatively correlated with Sr/Y (Fig. 5), indicating that the adakitic magma interacted with a fluid-metasomatised mantle, which has been en route to the surface. Daisen is located about 400 km from the Nankai Trough, where the Philippine Sea Plate subducts beneath Shikoku. Because it is difficult to trace the configuration of the Plate, the depth to the subducting plate in this area is controversial. However, it is estimated to be at a depth of at least 60 km (Ueno *et al.*, 2008; Iidaka *et al.*, 2009). It is conceivable that P–T conditions for the subducting slab beneath Daisen volcano include passing through a hot stage at which slab melting starts. The estimated age of the subducting Philippine Sea Plate is, however, around 26–28 Myr, which is close to the boundary conditions at which slab melting can happen. When such an relatively old slab melts, dehydration might also take place due to subtle differences in P–T conditions at the locus of melting place. Alternatively, hydrated mantle might have been dragged down with the downward flow of the mantle wedge. The presence of radioactive disequilibrium with (^{238}U/^{230}Th) > 1, in any case, necessitates that fluid addition took place within 400 kyr before present.

Figure 6 shows trace element abundances of adakites from Quimsacocha (Beate *et al.*, 2001), Antisana (Bourdon *et al.*, 2002) in Ecuaror, Pirca Negras in Argentina (Goss and Kay, 2009), Cook Islands (Stern and Kilian, 1996) and Lautaro (Orihashi *et al.*, 2004, 2008) in Chile normalized to N-MORB (Sun and McDonough,

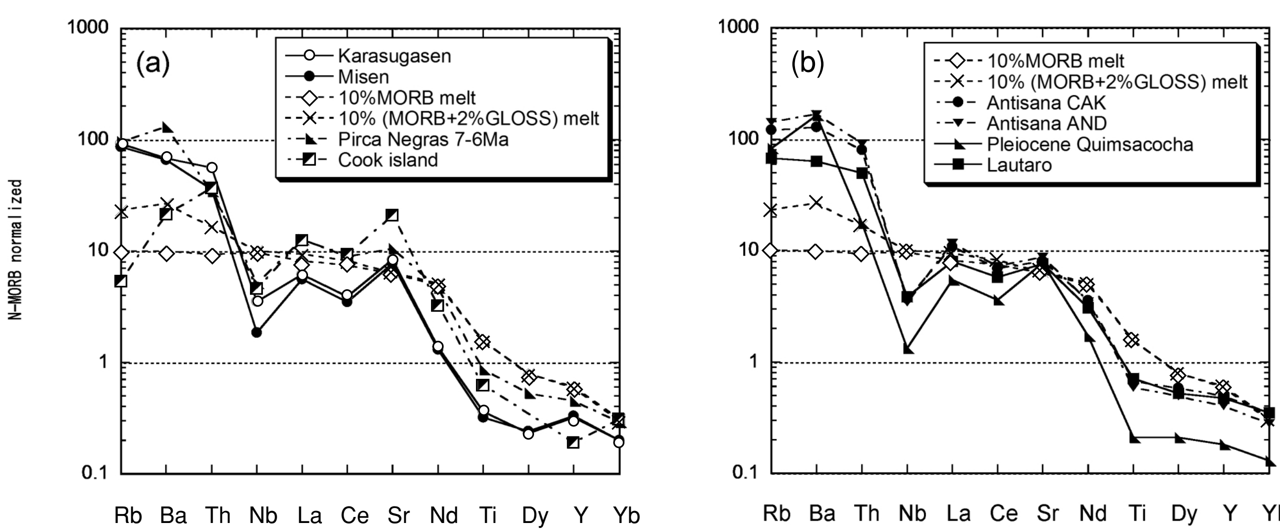

Fig. 6. N-MORB normalized trace element abundance patterns of adakites. Model calculations for 10% MORB melt and 10% melt of a mixture of MORB and GLOSS sediment were done following the method of Stracke et al. (2003). Trace element data of the Quimsacocha, Antisana, Pirca Negras, Cook Islands, and Lautaro are respectively referred from Beate et al. (2001), Bourdon et al. (2002), Goss and Kay (2009), Stern and Kilian (1996) and Orihashi et al. (2004, 2008).

1989). Results of calculations using a model of 10% batch partial melting of N-MORB and 10% melt of a mixture of N-MORB and 2% sediment (GLOSS, Plank and Langmuir, 1998) are also shown. Partition coefficients for eclogite (Stracke *et al.*, 2003) were used for the calculation. The order of the elements has been arranged according to decreasing magnitude of the partition coefficients that operate during generation of oceanic basalts. Among the four elements at the far left, Rb and Ba are fluid mobile, while Th and Nb are fluid immobile. Although trace element abundances of adakites will change according to several factors such as the degree of melting, residual phases during melting and intra-crustal differentiation, the comparison of the patterns formed by the four elements with those of two results of the calculations is still useful to gauge the influence of fluid-related metasomatism qualitatively. The N-MORB normalized trace element pattern (Fig. 6) of samples from Misen edifice of Daisen shows enrichment in Rb and Ba than the N-MORB melts with or without sediment. Possibly, the sub-crustal mantle beneath Misen edifice has suffered hydrous metasomatism. Meanwhile, the trace element pattern of samples from Karasugasen edifice shows enrichment also in fluid immobile elements, such as Th and Nb, suggesting enrichment mechanism may be different for the two eddifices.

Available data related to U–Th radioactive disequilibria of adakites remain limited. The abundance ratios of large ion lithophile elements (LILE) to fluid immobile elements, such as Rb/Nb, provide useful indices for detecting contribution of slab-derived fluid to magma generation in island-arc environments. The Rb/Nb ratio of the samples from Misen, with averages of 11.6, is higher than that from Karasugasen, with averages of 6.4, despite some overlap. Although adakites with high Rb/Nb more than ten are observed in the Aleutians (Kamber *et al.*, 2002), Mindanao (Sajona *et al.*, 1997), Negros Arc (Solidum *et al.*, 2003), central Luzon (Yumul *et al.*, 2003), and several volcanoes in Ecuador, it is uncommon to find adakites with high Rb/Nb existing with those having low ratios. Contemporary eruption of the two types of adakites is limited to Antisana in Ecuador. Average compositions for adakites from the Cook Islands, Viedma, Aguilera and Reclus of the Austral Volcanic Zone in Chile, with large excess of (^{230}Th) over (^{238}U) (Fig. 4) are clearly depleted in Rb and Ba. The average of Rb/Nb ratio of the volcanoes is 4.8. Comparing adakites from different volcanoes, the sources of adakites from Misen have apparently experienced fluid-related metasomatism to a greater extent. Pleiocene adakites from Quimsacocha, Ecuador, and 6–7 Ma adakites from Pirca Negras, Ecuador show similar enrichments in Rb and Ba.

The above discussions do not consider the influence of crustal assimilation. Rb in particular is susceptible to modification by the process. Higher Rb/Nb ratio of adakites from Misen than those from Karasugasen, however, can mostly be attributed to fluid addition process, because the large extent of lower crustal assimilation would have lowered (^{230}Th/^{232}Th), which contradicts the observed relation between the adakites from the two domes (Fig. 4).

Our new finding of adakites with (^{238}U) excess over (^{230}Th), together with compilation of adakites from other areas, might indicate that even where warm subduction is taking place, the hydrate layer can be downdragged to adakitic-magma generation depths in the bottom of mantle wedge. Or it might indicate that when an relatively old slab melts, dehydration might also take place in proximity to where melting occurs.

Acknowledgments—This research was partly supported by grants in aid for Scientific Research from Japan Society for the Promotion of Science to SN. We thank Y. Nishio for technical assistance and Y. Maeda, S. Fukuda and T. Kusano for their help during field work. We thank valuable comments from P. Morris, H. Iwamori, and an anonymous reviewer.

References

Atherton, M. P. and Petford, N. (1993) Generation of sodium-rich magmas from newly underplated basaltic crust. *Nature* **362**, 144–146.

Beate, B., Monzier, M., Spikings, R., Cotton, J., Silva, J., Bourdon, E. and Eissen, J. P. (2001) Mio–Pleiocene adakite generation related to flat subduction in southern Ecuador: the Quimsacocha volcanic center. *Earth Planet. Sci. Lett.* **192**, 561–570.

Beattie, P. (1993) Uranium–thorium disequilibria and partitioning on melting garnet peridotite. *Nature* **363**, 63–65.

Bourdon, E., Eissen, J. P., Monzier, M., Rovin, C., Martin, H., Cotten, J. and Hall, M. L. (2002) Adakite-like lavas from Antisana volcano (Ecuador): Evidence for slab melt metasomatism beneath the Andean Northern Volcanic Zone. *J. Petrol.* **43**, 199–217.

Cheng, H., Edwards, R. L., Hoff, J., Gallup, C. D., Richards, D. A. and Asmerom, Y. (2000) The half lives of uranium-234 and thorium-230. *Chem. Geol.* **169**, 17–33.

Defant, M. J. and Drummond, M. S. (1990) Derivation of some modern arc magmas by melting of young subducted lithosphere. *Nature* **347**, 662–665.

Defant, M. J. and Drummond, M. S. (1993) Mount St. Helens: Potential example of the partial melting of the subducted lithosphere in a volcanic arc. *Geology* **21**, 547–550.

Defant, M. J., Richerson, P. M., De Boer, J. Z., Stewart, R. H., Maury, R. C., Bellon, H., Drummond, M. S., Feigenson, M. D. and Jackson, T. E. (1991) Dacite genesis via both slab melting and differentiation: Petrogenesis of La Yeguada Volcanic Complex, Panama. *J. Petrol.* **32**, 1101–1142.

Drummond, M. S. and Defant, M. J. (1990) A model for trondhjemite-tonalite-dacite genesis and crustal growth via slab melting; Archean to modern comparisons. *J. Geophys. Res.* **95**, 21503–21521.

Fukuda, S. and Nakai, S. (2002) $^{238}U/^{230}Th$ disequilibrium measurement for volcanic rock samples using a multiple-collector ICPMS. *Geochem. J.* **36**, 465–473.

Fukuda, S., Nakai, S., Niihori, K., Tsukui, M., Nakada, S., Fujii, T. and Tani, K. (2008) ^{238}U–^{230}Th radioactive disequilibrium in the northern Izu arc: ($^{230}Th/^{232}Th$) in the sub-arc mantle. *Geochem. J.* **42**, 461–479.

Goss, A. R. and Kay, S. M. (2009) Extreme high field strength element (HFSE) depletion and near-chondritic Nb–Ta ratios in Central Andean adakite-like lavas (~28S, ~68W). *Earth Planet. Sci. Lett.* **279**, 97–109.

Holden, N. E. (1990) Total half-lives for selected nuclides. *Pure Appl. Chem.* **62**, 941–958.

Iidaka, T., Igarashi, T. and Iwasaki, T. (2009) Configuration of the subducting Philippine Sea slab in the eastern part of southwestern Japan with seismic array and Hi-net data. *Gondwana Res.* **16**, 504–511.

Iwamori, H. (1991) Zonal structure of Cenozoic basalts related to mantle upwelling in southwest Japan. *J. Geophys. Res.*, **96**(B4), 6157–6170.

Jaffey, A., H., Flynn, K. F., Glendenin, L. E., Bentley, W. C. and Essling, A. M. (1971) Precision measurement of half-lives and specific acitivities of ^{235}U and ^{238}U. *Phys. Rev.* **C4**, 1889.

Kamber, B. S., Ewart, A., Collerson, K. D., Bruce, M. C. and McDonald, G. D. (2002) Fluid-mobile trace element constraints on the role of slab melting and implications for Archaean crustal growth models. *Contrib. Mineral. Petrol.* **144**, 38–56.

Kimura, J., Tateno, M. and Osaka, I. (2005) Geology and geochemistry of Karasugasen lava dome, Daisen–Hiruzen Volcano Group, southwest Japan. *Island Arc* **14**, 115–136.

LaTourette, T. K., Kennedy, A. K. and Wasserburg, G. J. (1993) Thorium–uranium fractionation by garnet: evidence for a deep source and rapid rise of oceanic basalts. *Science* **261**, 739–742.

Martin, H. (1986) Effect of steeper Archaean geothermal gradient on geochemistry of subduction-zone magmas. *Geology* **14**, 753–756.

Martin, H. (1999) Adakitic magmas: modern analogues of Archaean granitoids. *Lithos* **46**, 411–429.

McDonough, W. F. and Sun, S. S. (1995) The composition of the Earth. *Chem. Geol.* **120**, 223–253.

Morris, P. A. (1995) Slab melting as an explanation of Quaternary volcanism and aseismicity in southwest Japan. *Geology* **23**, 395–398.

Orihashi, Y., Naranjo, J. A., Motoki, A., Sumino, H., Hirata, D., Anma, R. and Nagao, K. (2004) Quaternary volcanic activity of Hudson and Lautaro volcanoes, Chilean Patagonia: new constraints from K–Ar ages. *Rev. Geol. Chile* **31**, 207–224.

Orihashi, Y., Nakai, S., Shinjoe, H., Naranjo, J. A., Motoki, A. and CHRISTMASSY Group (2008) Magmatic evolution of the Quaternary volcanics from Hudson and Lautaro volcanoes, Austral Andean Cordillera. *18th Goldschmidt Conference, Vancouver, Canada, July 13–18, Geochim. Cosmochim. Acta Spec. Suppl.*, A709.

Peacock, S. M. and Wang, K. (1999) Seismic consequences of warm versus cool subduction metamorphism: examples from southwest and northeast Japan. *Science* **286**, 937–942.

Plank, T. and Langmuir, C. H. (1998) The chemical composition of subducting sediment and its consequences for the crust and mantle. *Chem. Geol.* **145**, 325–394.

Rudnick, R. L. and Gao, S. (2003) Composition of the continental crust. *Treatise on Geochemistry 3* (Rudnick, R. L., ed.), 1–64, Elsevier.

Sajona, F. G., Bellon, H., Maury, R. C., Pubellier, M., Quebral., R. D., Cotten, J., Bayon, F. E., Pagadog, E. and Pamatian, P. (1997) Tertiary and Quaternary magmatism in Mindanao and Leyte (Philippines): geochronology, geochemistry and tectonic setting. *J. Asian Earth Sci.* **15**, 121–153.

Shiomi, K., Obara, K. and Sato, H. (2006) Moho depth variation beneath southwestern Japan revealed from the velocity structure based on receiver function inversion. *Tectonophysics*, **420**, 205–221.

Sigmarsson, O., Martin, H. and Knowles, J. (1998) Melting of a subducting oceanic crust from U–Th disequilibria in austral Andean lavas. *Nature* **394**, 566–569.

Solidum, R. S., Castillo, P. R. and Hawkins, J. W. (2003) Geochemistry of lavas from Negros Arc, west central Philippines: Insights into the contribution from the subducting slab. *Geochem. Geophys. Geosys.* 9008, doi:10.1029/2003GC000513.

Stern, C. R. and Kilian, R. (1996) Role of the subducted slab, mantle wedge and continental crust in the generation of adakites from the Andean Austral Volcanic Zone. *Contrib. Mineral. Petrol.* **123**, 263–281.

Stracke, A., Bizimis, M. and Salters, V. J. M. (2003) Recycling oceanic crust: Quantitative constraints. *Geochem. Geophys. Geosys.* **4**, doi:10.1029/2001GC000223.

Sun, S.-S. and McDonough, W. F. (1989) Chemical and isotopic systematics of oceanic basalts: implications for mantle composition and processes. *Magmatism in the Ocean Basins, Geological Society Spec. Publ. 42* (Saunders, A. D. and Norry, M. J., eds.), 313–345, Oxford.

Tamura, Y., Yuhara, M. and Ishii, T. (2000) Primary arc basalts from Daisen volcano, Japan: equilibrium crystal fractionation versus disequilibrium fractionation during supercooling. *J. Petrol.* **41**, 431–448.

Tamura, Y., Yuhara, M., Ishii, T., Irino, N. and Shukuno, H. (2003) Andesites and dacites from Daisen volcano, Japan: partial-to-total melting of an andesite magma body. *J. Petrol.* **44**, 2243–2260.

Tani, K., Orihashi, Y. and Nakada, S. (2002) Major and trace component analysis of silicate rocks using fused glass bead by X-ray fluorescence spectrometer: Evaluation of analytical precision for third, sixth and eleventh dilution fused glass beads. *Technical Research Report, ERI, University of Tokyo* **8**, 26–36 (in Japanese with English abstract).

Tsukui, M. (1984) Geology of Daisen volcano. *J. Geol. Soc. Jpn.* **90**, 643–658.

Tsukui, M. (1985) Temporal variation in chemical composition of phenocrysts and magmatic temperature at Daisen volcano, southwest Japan. *J. Volcanol. Geotherm. Res.* **26**, 317–336.

Tsukui, M., Nishido, H. and Nagao, K. (1985) K–Ar ages of the Hiruzen volcano group and the Daisen volcano. *J. Geol. Soc. Jpn.* **91**, 279–288.

Turner, S., Bourdon, B. and Gill, J. (2003) Insights into magma genesis at convergent margins from U-series isotopes. *Rev. Mineral. Geochem.* **52**, 255–315.

Ueno, T., Shibutani, T. and Ito, K. (2008) Configuration of the continental Moho and Philippine Sea slab in southwest Japan derived from receiver function analysis: relation to subcrustal earthquakes. *Bull. Seismol. Soc. Amer.* **98**, 2416–2427.

Yumul, G. P., Jr., Carla, B. D, Tamayo, R. A., Jr. and Bellon, H. (2003) Silicic arc volcanism in central Luzon, the Philippines: characterization of its space, time and geochemical relationship. *Island Arc*, **12**, 207–218.

Zindler, A. and Hart, S. R. (1986) Chemical geodynamics. *Annu. Rev. Earth Planet. Sci.* **14**, 493–571.

APPENDIX

Appendix 1. Major and trace element abundances and abundance ratio of Daisen adakites

Dome	Karasugasen							Misen					
Sample No.	K1	K2	K3	K4	K5	K7	K11	M1	M2	M3	M6	M7	M10
SiO_2 (wt%)	62.69	63.90	64.54	64.17	65.12	64.64	64.72	64.41	64.81	65.49	64.19	64.33	65.24
TiO_2 (wt%)	0.47	0.44	0.43	0.47	0.43	0.45	0.47	0.47	0.42	0.04	0.47	0.42	0.43
Al_2O_3 (wt%)	18.03	17.28	17.32	17.06	16.88	16.97	16.89	17.11	17.09	17.16	16.88	17.38	16.95
Fe_2O_3 (wt%)	4.36	3.94	3.84	4.11	4.19	4.03	4.14	4.28	4.08	3.97	4.02	4.01	4.01
MnO (wt%)	0.08	0.07	0.07	0.07	0.08	0.07	0.07	0.08	0.08	0.08	0.07	0.07	0.08
MgO (wt%)	2.21	2.03	1.97	2.20	1.93	2.01	2.11	2.02	1.88	1.73	1.99	1.84	1.82
CaO (wt%)	4.59	4.66	4.52	4.50	4.78	4.48	4.41	4.82	4.87	4.84	4.81	4.90	4.71
Na_2O (wt%)	4.27	4.50	4.55	4.46	4.28	4.50	4.37	4.30	4.29	4.34	4.34	4.44	4.33
K_2O (wt%)	1.59	1.98	2.01	2.05	1.76	2.05	2.01	1.78	1.72	1.71	2.05	1.83	1.79
P_2O_5 (wt%)	0.14	0.20	0.18	0.19	0.14	0.22	0.20	0.14	0.14	0.14	0.19	0.13	0.15
Sc (ppm)	11	9	9	9	10	9	11	10	10	9	9	9	9
V (ppm)	76	65	72	58	66	57	76	67	65	64	67	67	73
Cr (ppm)	16	14	15	16	18	16	14	18	17	17	16	16	16
Co (ppm)	11	11	9	12	10	11	12	10	10	10	10	10	9
Ni (ppm)	16	16	15	17	9	16	16	10	9	9	16	12	10
Rb (ppm)	45	55	55	58	49	55	54	49	47	47	55	51	50
Sr (ppm)	755	820	805	788	666	792	752	688	692	688	907	717	697
Y (ppm)	9	9	9	9	9	9	9	9	9	9	10	8	10
Zr (ppm)	134	135	134	137	119	144	134	120	113	113	126	110	112
Nb (ppm)	8	9	9	10	5	10	9	5	4	4	6	4	4
Ba (ppm)	401	423	432	451	423	446	440	442	419	400	471	401	425
Pb (ppm)	8	7	8	9	8	12	8	8	7	10	6	7	8
Th (ppm)	9	9	6	10	5	9	7	3	3	5	5	5	5
Sr/Y	86	94	92	89	73	86	82	78	76	79	94	86	73

Abundances were measured by XRF.

Appendix 2. REE abundances of Daisen adakites

Dome	Karasugasen				Misen			
Sample No.	K1	K4	K5	K7	M1	M2	M3	M4
La	13.0	18.7	9.65	20.2	19.4	11.1	11.4	12.0
Ce	28.4	33.7	18.1	37.5	35.5	20.5	22.1	23.4
Pr	2.57	3.29	1.87	3.92	3.72	2.18	2.26	2.47
Nd	8.93	10.9	6.61	13.5	12.9	7.63	7.87	8.67
Sm	1.58	1.74	1.22	2.25	2.20	1.38	1.37	1.55
Eu	0.582	0.642	0.605	0.724	0.738	0.656	0.648	0.657
Gd	1.24	1.26	0.982	1.68	1.63	1.09	1.06	1.22
Tb	0.180	0.179	0.154	0.235	0.233	0.165	0.160	0.183
Dy	1.01	0.994	0.928	1.33	1.32	0.997	0.948	1.08
Ho	0.197	0.197	0.187	0.257	0.257	0.198	0.191	0.212
Er	0.563	0.554	0.554	0.713	0.711	0.566	0.557	0.614
Tm	0.083	0.085	0.086	0.105	0.104	0.088	0.084	0.094
Yb	0.549	0.564	0.583	0.693	0.677	0.589	0.589	0.625
Lu	0.082	0.087	0.092	0.103	0.100	0.092	0.089	0.097